# Natural convection in rectangular enclosures partially filled with a porous medium

**T. W. Tong* and E. Subramanian†**

Analysis is undertaken of steady-state natural convection heat transfer in rectangular enclosures, that are vertically divided into a region filled with a fluid and another filled with a fluid-saturated porous medium. The two are separated by an impermeable wall and the vertical and horizontal boundaries are considered to be isothermal and adiabatic, respectively. The objective is to establish the heat transfer characteristics for enclosures containing different amounts of porous material. The flow in the porous region is modelled by a modified Darcy's law where Brinkman's extension is incorporated to allow the no-slip condition to be satisfied. A finite-difference scheme was used to numerically solve the field equations in the two regions. It was found that there were situations where heat transfer could be minimized by partially filling instead of entirely filling an enclosure with a porous medium. Results obtained in this study are directly applicable to the design of insulation systems, suggesting that a better optimized insulation usage is possible.

**Keywords:** *natural convection, porous medium, enclosure, insulation*

One effective method to suppress convective heat transfer in an enclosure is to fill it with a porous material. The solid matrix usually occupies only a small fraction of the enclosed space; but because of its very fine structure, the total surface available for frictional resistance is large enough to significantly retard the fluid motion. An example of this can be found in home insulation where the air space between wall panels is filled with a light-weight fibreglass insulation ($\sim 10\ \mathrm{kg/m^3}$).

In many situations, it is common to entirely fill the enclosure with a porous material when insulation is desired. The aim of this work is to study the effect of partially rather than completely filling an enclosure with a porous insulation. From an engineering standpoint, the motivation for performing such an analysis is obvious. If the insulation usage is better optimized, the potential savings in capital as well as operating costs of the insulation system could be appreciable. The particular problem considered here is idealized as 2-D and rectangular with isothermal vertical and insulated horizontal boundaries (see Fig 1). The enclosed space is considered to be vertically divided into two regions with one filled with a porous medium. An impermeable surface, simulating the paper-backing or the vapour barrier of the insulation, separates the two regions. Thus, in effect the problem examined is one of two enclosures sharing a common vertical boundary.

* Department of Mechanical Engineering, University of Kentucky, Lexington, KY 40506, USA
† Presently, with Probe Technology, Santa Clara, CA 95054, USA
Received 23 July 1985 and accepted for publication in final form on 2 October 1985

A review of the literature related to heat transfer in rectangular enclosures shows that previous analyses can be classified mainly into three categories: (i) those that concern fluid-filled enclosures[1-7], (ii) those that concern porous-filled enclosures[7-15] and (iii) those that consider a partition separating either two fluid media[16-17] or two porous media[18,19]. The present problem does not fall into any of these three classes of problems. But in the limiting cases of zero insulation thickness and an enclosure entirely filled with an insulation, the problem would belong to either one of the first two categories described above.

## Mathematical formulation

Shown in Fig 1 is the geometry of the problem under consideration. The region between the hot boundary and the impermeable partition is filled with a porous medium saturated with the same fluid that occupies the rest of the enclosure. For constant properties (except the density in the buoyancy term) and steady-state free convection, the equations governing the conservation of mass, momentum and energy in each of the two regions have been well established[7]. Instead of repeating all the equations in their dimensional form, we shall only cover those that are different from the traditional formulation[7] and present the final dimensionless equations. It should be noted that for porous media comprised of loose-fill materials such as packed-glass spheres, the porosity variation near a solid surface may have a significant effect on energy transfer and the constant properties assumption may need to be modified accordingly[20].

In the present analysis Brinkman's extension[21] has been incorporated in the conventional Darcy formulation for momentum transfer in a porous medium. The modified Darcy's law can be written as:

$$\frac{\mu_f}{\kappa}\bar{u}_p = -\frac{\partial P_p}{\partial \bar{x}} + \mu_p\left(\frac{\partial^2 \bar{u}_p}{\partial \bar{x}^2} + \frac{\partial^2 \bar{u}_p}{\partial \bar{y}^2}\right) \tag{1}$$

$$\frac{\mu_f}{\kappa}\bar{v}_p = -\frac{\partial P_p}{\partial \bar{y}} + \mu_p\left(\frac{\partial^2 \bar{v}_p}{\partial \bar{x}^2} + \frac{\partial^2 \bar{v}_p}{\partial \bar{y}^2}\right) + \rho g \beta (T_p - T_m) \tag{2}$$

where the symbols are defined under Notation. The bars distinguish the respective variables from their dimensionless counterparts to be used later. It is seen that Brinkman's extension includes the shear stress terms in the original Darcy's law allowing the no-slip boundary condition to be satisfied. The reason for using Brinkman's extension is because the present analysis is related to another investigation being conducted by the authors. This other investigation considers no solid surface separating the porous and the fluid regions. That is, the fluid in the porous side can flow to the fluid side and vice versa. In such a situation, Brinkman's extension may be necessary for the shear stress matching condition at the porous-fluid interface to be satisfied. To allow a more compatible comparison of the results in the future, it was decided to have a consistent formulation for both the present problem with a solid interface and the other problem without a solid interface.

It should be noted that $\mu_p$ and $\mu_f$ are generally different from one another. However, the simplification of treating $\mu_p = \mu_f$ has been found acceptable for many situations[21-24]. Adopting this simplification, using the following dimensionless variables:

$$x = \frac{\bar{x}}{d}, \quad y = \frac{\bar{y}}{d}, \quad \theta_p = \frac{T_p - T_c}{T_h - T_c}, \quad \theta_f = \frac{T_f - T_c}{T_h - T_c}$$

$$u_p = \frac{\bar{u}_p d}{\alpha_p}, \quad v_p = \frac{\bar{v}_p d}{\alpha_p}, \quad u_f = \frac{\bar{u}_f d}{\alpha_f}, \quad v_f = \frac{\bar{v}_f d}{\alpha_f}$$

$$Ra_o = \frac{\rho g \beta (T_h - T_c)\kappa d}{\mu_f \alpha_p}, \quad Ra = \frac{\rho g \beta (T_h - T_c) d^3}{\mu_f \alpha_f}$$

$$Da = \frac{\kappa}{d^2}, \quad Pr = \frac{\mu_f}{\rho \alpha_f}$$

we transform Eqs (1) and (2), and the rest of the governing equations[7] to the following dimensionless form in terms of the stream functions:

### Porous region

$$\frac{\partial^2 \psi_p}{\partial x^2} + \frac{\partial^2 \psi_p}{\partial y^2} = Da\left(\frac{\partial^4 \psi_p}{\partial x^4} + 2\frac{\partial^4 \psi_p}{\partial x^2 \partial y^2} + \frac{\partial^4 \psi_p}{\partial y^4}\right) - Ra_o \frac{\partial \theta_p}{\partial x} \tag{3}$$

$$\frac{\partial \psi_p}{\partial y}\frac{\partial \theta_p}{\partial x} - \frac{\partial \psi_p}{\partial x}\frac{\partial \theta_p}{\partial y} = \frac{\partial^2 \theta_p}{\partial x^2} + \frac{\partial^2 \theta_p}{\partial y^2} \tag{4}$$

### Fluid region

$$\frac{\partial^3 \psi_f}{\partial x^3}\frac{\partial \psi_f}{\partial y} - \frac{\partial \psi_f}{\partial x}\frac{\partial^3 \psi_f}{\partial x^2 \partial y} + \frac{\partial \psi_f}{\partial y}\frac{\partial^3 \psi_f}{\partial x \partial y^2} - \frac{\partial \psi_f}{\partial x}\frac{\partial^3 \psi_f}{\partial y^3}$$
$$= Pr\left(\frac{\partial^4 \psi_f}{\partial x^4} + 2\frac{\partial^4 \psi_f}{\partial x^2 \partial y^2} + \frac{\partial^4 \psi_f}{\partial y^4}\right) - Ra\,Pr\frac{\partial \theta_f}{\partial x} \tag{5}$$

$$\frac{\partial \psi_f}{\partial y}\frac{\partial \theta_f}{\partial x} - \frac{\partial \psi_f}{\partial x}\frac{\partial \theta_f}{\partial y} = \frac{\partial^2 \theta_f}{\partial x^2} + \frac{\partial^2 \theta_f}{\partial y^2} \tag{6}$$

The dimensionless parameters $Ra_o$, $Ra$, $Da$ and $Pr$ are respectively, the modified Rayleigh number, the Rayleigh number, the Darcy number and the Prandtl number. The dimensionless variables shown above are chosen such that Eqs (3) (without Brinkman's extension) and (4), and Eqs (5) and (6) are identical to those for porous-filled[7,9] and fluid-filled[7] enclosures, respectively.

The boundary conditions for the present problem are:

$$\text{at } x=0 \qquad \theta_p = 1, \quad \psi_p = 0, \quad \frac{\partial \psi_p}{\partial x} = 0 \tag{7}$$

$$\text{at } x=1 \qquad \theta_f = 0, \quad \psi_f = 0, \quad \frac{\partial \psi_f}{\partial x} = 0 \tag{8}$$

$$\text{at } y=0, A \quad \frac{\partial \theta_p}{\partial y} = 0, \quad \psi_p = 0, \quad \frac{\partial \psi_p}{\partial y} = 0 \quad \text{for } x < S \tag{9}$$

$$\frac{\partial \theta_f}{\partial y} = 0, \quad \psi_f = 0, \quad \frac{\partial \psi_f}{\partial y} = 0 \quad \text{for } x > S \tag{10}$$

## Notation

| | |
|---|---|
| $A$ | Aspect ratio |
| $d$ | Width of the enclosure |
| $g$ | Gravitational acceleration |
| $k_f$ | Thermal conductivity of the fluid |
| $k_p$ | Thermal conductivity of the porous medium |
| $L$ | Height of the enclosure |
| $M$ | Number of intervals in the porous region in the $x$ direction |
| $N$ | Number of intervals in the fluid region in the $x$ direction |
| $Nu$ | Nusselt number, see definition in Eq (14) |
| $P$ | Perturbation pressure, also number of intervals in the $y$ direction |
| $Pr$ | Prandtl number |
| $R$ | $R_c$ for $x \leqslant S$ and unity for $x \geqslant S$ |
| $R_c$ | Ratio of $k_f$ to $k_p$ |
| $Ra$ | Rayleigh number |
| $Ra_o$ | Modified Rayleigh number |
| $s$ | Width of the porous region |
| $S$ | Dimensionless width of the porous region |
| $T$ | Temperature |
| $\bar{u}$ | Horizontal velocity |
| $u$ | Dimensionless horizontal velocity |
| $\bar{v}$ | Vertical velocity |
| $v$ | Dimensionless vertical velocity |
| $\bar{x}$ | Horizontal coordinate |
| $x$ | Dimensionless horizontal coordinate |
| $\bar{y}$ | Vertical coordinate |
| $y$ | Dimensionless vertical coordinate |
| $\alpha$ | Thermal diffusivity |
| $\beta$ | Thermal expansion coefficient |
| $\theta$ | Dimensionless temperature |
| $\kappa$ | Permeability |
| $\mu_f$ | Viscosity of the fluid |
| $\mu_p$ | Effective viscosity of the porous medium |
| $\rho$ | Density of the fluid |
| $\psi$ | Dimensionless stream function |

*Subscripts*

| | |
|---|---|
| c | Cold wall |
| f | Fluid |
| h | Hot wall |
| m | Mean |
| p | Porous medium |

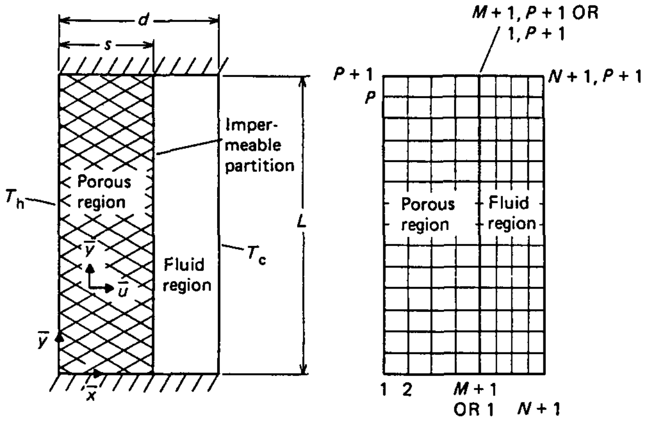


*Fig 1 Enclosure partially filled with a porous medium: (a) physical geometry; (b) grid pattern*

where $A$ and $S$ are defined as:

$$A=\frac{L}{d}, \qquad S=\frac{s}{d}$$

The appropriate matching conditions at the solid interface are:

$$\text{at } x=S \qquad \theta_p=\theta_f, \quad \frac{\partial\theta_p}{\partial x}=R_c\frac{\partial\theta_f}{\partial x}$$

$$\psi_p=\psi_f=0, \quad \frac{\partial\psi_p}{\partial x}=\frac{\partial\psi_f}{\partial x}=0 \tag{11}$$

where $R_c=k_f/k_p$. It should be noted that $Ra_o$, $Ra$, $Da$ and $R_c$ are related by:

$$Ra_o=Ra\, Da\, R_c \tag{12}$$

Therefore, only three of the parameters appearing in Eq (12) are independent.

## Method of solution

In view of the mathematical complexity involved in the equations, a numerical solution was attempted. The entire enclosure was divided to a $(M+N)\times P$ grid with $M$ and $N$ corresponding to the numbers of intervals in the porous and fluid sides, respectively, in the $x$ direction (see Fig 1b). Central-differences with second order accuracy were used to transform the governing equations to a set of algebraic equations. To maintain the same order of numerical accuracy, one-sided three point differences were employed at the solid boundaries. The procedure was iterative in nature where the stagnant conditions were taken as the initial state. Both the stream function and the temperature were iterated at every grid point until convergence was achieved.

The finite-difference forms of Eqs (3) and (5) were used to solve for the stream functions at locations at least two grid points away from any solid surfaces. For the points at and next to a boundary, the zero stream function and no-slip boundary conditions were applied, respectively. As far as temperature was concerned, the finite-difference forms of Eqs (4) and (6) were employed for all interior grid points while the thermal conditions specified in Eqs (7) to (10) were applied along the enclosure boundaries. Combining the thermal matching conditions shown in Eq (11) resulted in an algebraic equation that allowed the solid interface temperature to be determined in terms of the immediate neighbouring points in both the fluid and porous regions.

The convergence criterion was set by requiring the change of both the stream functions and temperatures at all grid points to be less than 0.01%. Other than those specified, the results reported were obtained with a $(16+16)\times 16$ grid. Test cases were conducted with finer grid points to ensure that the results would not change by more than 2.5% upon further reduction in grid size. The results for the test cases will also be presented in the next section.

## Results and discussion

In this work the governing parameters used in the calculations are intended to cover applications involving the use of highly porous (porosity $\geqslant 95\%$) insulations in moderate temperatures ($T_m \sim 300$ K, $(T_h-T_c)\leqslant 30$ K). The $Pr$ used throughout was 0.7 which is that for air at 300 K. Heat transfer results are presented as Nusselt number $Nu$ defined as:

$$Nu\equiv\frac{\text{actual head transfer}}{\text{heat transfer by conduction when the entire enclosure is filled with the fluid alone}} \tag{13}$$

In terms of the variables used, it is:

$$Nu=-\frac{1}{AR}\int_0^A\left(\frac{\partial\theta}{\partial x}-\theta u\right)dy \tag{14}$$

where:

$$R=R_c, \quad \theta=\theta_p, \quad u=u_p \quad \text{for } x\leqslant S$$
$$R=1, \quad \theta=\theta_f, \quad u=u_f \quad \text{for } x\geqslant S$$

Normally, $Nu$ is defined with the denominator equal to the conductive heat transfer across the actual enclosure. But since here we are considering enclosures that have physically different geometries (corresponding to different values of $S$), it is more suitable to have all the $Nu$ defined on the same basis, as in Eq (13), to facilitate comparisons of results. A simple analysis can show that in the conduction limit, the present definition of $Nu$ gives:

$$Nu=1/[1+S(R_c-1)] \tag{15}$$

Therefore only for the special case of $R_c=1$ will the present and the conventional $Nu$ have the same limiting value of one. All the $Nu$ presented were evaluated at $x=0$ although $Nu$ at both the hot and cold walls were computed in the analysis. Typically, the $Nu$ determined at both walls differ by no more than 2%.

Given in Tables 1 and 2 are some results illustrating the effect due to different grid sizes. Most of the results obtained with a $(16+16)\times 16$ grid did not change by more than 2.5% upon incrementing each of the grid intervals by 4. For cases where $Nu$ changed by more than 2.5%, more tests were performed by increasing the grid intervals further. The tests show that there are cases which will require a $(20+20)\times 20$ grid for the results to be considered as grid-size independent. Also included in Tables 1 and 2 are some numerical results reported by Raithby and Wong[6] for the case of $S=0$. All of the results that did not change by more than 2.5% upon further

**Table 1 Effect of grid size for $Ra=1\times10^4$ and $Da=1\times10^{-3}$**

| | | *Nu* | | |
|---|---|---|---|---|
| *S* | Grid pattern | *A*=5 | *A*=10 | *A*=20 |
| 0 | (0+16)×16 | 1.917 | 1.592 | 1.307 |
| | (0+20)×20 | 1.945 1.46* | 1.614 1.38 | 1.321 1.07 |
| | | (2.00)† | (1.67) | (1.37) |
| 0.1 | (16+16)×16 | 1.565 | | |
| | (20+20)×20 | 1.586 1.34 | | |
| 0.2 | (16+16)×16 | 1.309 | | |
| | (20+20)×20 | 1.318 0.69 | | |
| 0.3 | (16+16)×16 | 1.137 | | |
| | (20+20)×20 | 1.141 0.35 | | |
| 0.4 | (16+16)×16 | 1.044 | | |
| | (20+20)×20 | 1.047 0.29 | | |
| 0.5 | (16+16)×16 | 1.010 | 1.003 | 1.001 |
| | (20+20)×20 | 1.011 0.10 | 1.003 0.00 | 1.001 0.00 |
| 0.6 | (16+16)×16 | 1.003 | | |
| | (20+20)×20 | 1.003 0.00 | | |
| 0.7 | (16+16)×16 | 1.003 | | |
| | (20+20)×20 | 1.003 0.00 | | |
| 0.8 | (16+16)×16 | 1.005 | | |
| | (20+20)×20 | 1.006 0.10 | | |
| 0.9 | (16+16)×16 | 1.010 | | |
| | (20+20)×20 | 1.012 0.20 | | |
| 1.0 | (16+0)×16 | 1.017 | 1.006 | 1.002 |
| | (20+0)×20 | 1.019 0.20 | 1.007 0.10 | 1.002 0.00 |

* *Columns to the right of* Nu values contain the percent change from the preceding grid size in each case
† *The row of* Nu *values in parentheses is from Raithby and Wong*[6]

reduction in grid size agree with the cited results[6] to within 6%. For most cases, the agreement is better than 4%.

The results in Fig 2 are for $Ra_0$ of the order of $10^{-2}$. It is clear that most of the reduction in heat transfer occurs when $S \leqslant 0.6$. Depending on $R_c$, heat transfer may increase, decrease or remain the same when $S$ is further increased. This is because, for $Ra_0$ as low as $10^{-2}$, natural convection in the porous medium is negligible[7]. In addition, fluid circulation in the fluid region is suppressed as the fluid region is becoming more slender. Hence, heat transfer takes place largely by conduction once $S$ has reached 0.6. If $R_c < 1$ and $S$ is further increased, more of the fluid in the fluid region is replaced with a material that has a higher thermal conductivity and results in an increase in heat transfer. A statement in the opposite sense can be used to explain the monotonic decreasing trend for $R_c > 1$. For $R_c = 1$, the fluid and the porous medium are identical as far as conduction is concerned. Thus, there is no change in $Nu$ when $S$ is roughly greater than 0.6. The results for $R_c \leqslant 1$ are particularly relevant to insulation applications because most porous insulations have an $R_c$ either smaller than or close to one. It is obvious that the most desirable insulating effect can be achieved by partially filling instead of entirely filling the enclosure with a porous material.

Presented in Fig 3 are the vertical velocity and temperature distributions for $R_c = 1$ and the same $Ra$ and

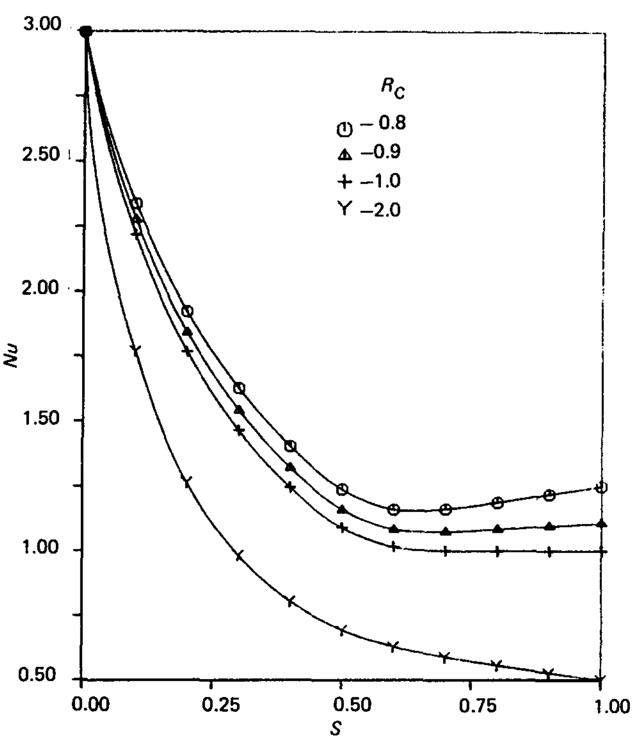


*Fig 2 Nusselt number for* $A = 10$, $Ra = 1 \times 10^5$ *and* $Da = 1 \times 10^{-7}$

**Table 2 Effect of grid size for $Ra=1\times10^5$ and $Da=1\times10^{-3}$**

| $S$ | Grid pattern | $Nu$ $A=5$ | $Nu$ $A=10$ | $Nu$ $A=20$ |
|---|---|---|---|---|
| 0 | (0+16)×16 | 3.425 | 2.994 | 2.500 |
| | (0+20)×20 | 3.524 2.89* | 0.039 1.50 | 2.544 1.76 |
| | (0+24)×24 | 3.580 1.59 | 3.067 0.92 | 2.562 0.71 |
| | | (3.68)† | (3.13) | (2.66) |
| 0.1 | (16+16)×16 | 2.498 | | |
| | (20+20)×20 | 2.551 2.12 | | |
| 0.2 | (16+16)×16 | 1.969 | | |
| | (20+20)×20 | 2.001 1.63 | | |
| 0.3 | (16+16)×16 | 1.637 | | |
| | (20+20)×20 | 1.657 1.22 | | |
| 0.4 | (16+16)×16 | 1.417 | | |
| | (20+20)×20 | 1.432 1.06 | | |
| 0.5 | (16+16)×16 | 1.264 | 1.128 | 1.050 |
| | (20+20)×20 | 1.278 1.11 | 1.138 0.89 | 1.055 0.48 |
| 0.6 | (16+16)×16 | 1.172 | | |
| | (20+20)×20 | 1.186 1.19 | | |
| 0.7 | (16+16)×16 | 1.169 | | |
| | (20+20)×20 | 1.185 1.37 | | |
| 0.8 | (16+16)×16 | 1.260 | | |
| | (20+20)×20 | 1.283 1.83 | | |
| 0.9 | (16+16)×16 | 1.426 | | |
| | (20+20)×20 | 1.460 2.38 | | |
| 1.0 | (16+0)×16 | 1.660 | 1.316 | 1.122 |
| | (20+0)×20 | 1.712 3.13 | 1.350 2.58 | 1.143 1.87 |
| | (24+0)×24 | 1.749 2.16 | 1.374 1.78 | 1.158 1.31 |
| | (32+0)×32 | 1.770 1.20 | 1.390 1.16 | |

* *Columns to the right of* Nu *values contain the percent change from the preceding grid size in each case*
† *The row of* Nu *values in parentheses is from Raithby and Wong*[6]

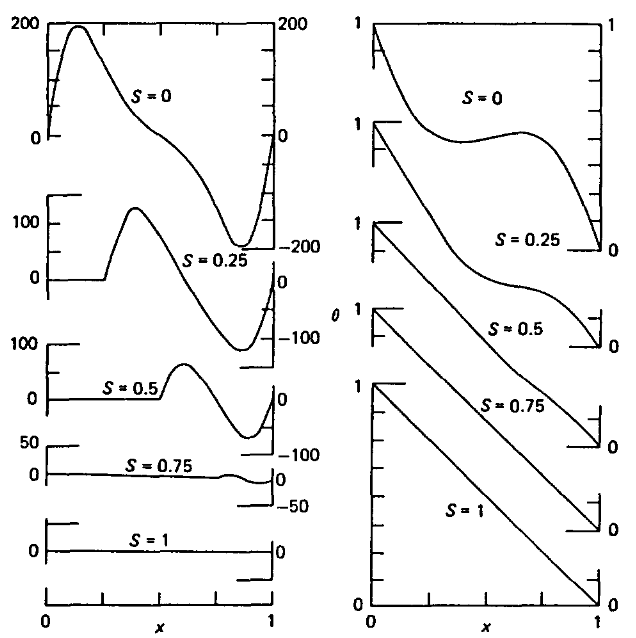


*Fig 3 Distributions at mid-height of the enclosure for* $A=10$, $Ra=1\times10^5$, $Da=1\times10^{-7}$ *and* $R_c=1$*: (a) vertical velocity; (b) temperature*

*Da* as in Fig 2. The effect on convection suppression can also be seen in this figure. When $S$ is increased from zero, there is no fluid motion in the region occupied by the porous medium and the velocity in the fluid side decreases substantially. The temperature distribution is becoming more linear indicating heat transfer is approaching the conduction limit. The profiles show that convection is already negligible when $S$ is somewhere between 0.5 and 0.75.

The $Nu$ for $R_c\leqslant1$ and $Ra_o$ of the order of $10^2$ are given in Fig 4. The results for $S=1$ were obtained with a $(20+20)\times20$ grid which was found necessary for the results not to change more than 2.5% upon further reduction in grid sizes. It is seen that all the results including those for $R_c=1$ exhibit a minimum around $S=0.65$. An examination of the vertical velocity and temperature distributions (see Fig 5) reveals that when $Ra_o$ is of the order of $10^2$, there is convection in both the porous and the fluid regions. The fluid motion is clearly minimized when $S$ is between 0.5 and 1. This is consistent with what is observed in Fig 4.

Figs 6 to 9 form a series of graphs giving $Nu$ for different $Ra$, $Da$ and $A$. A shorter enclosure and a larger $Ra$ have the same effect of increasing heat transfer. The value of $S$ beyond which there is either no change or increase in heat transfer is larger for lower $A$ and higher

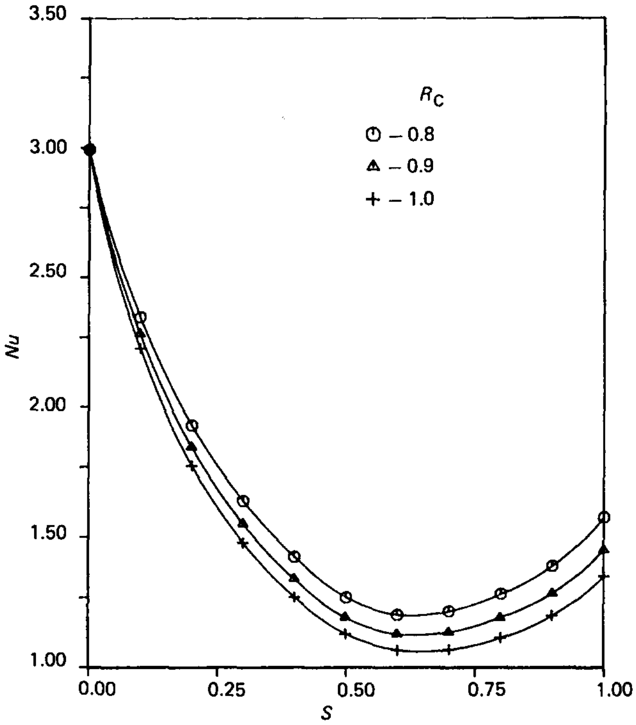


*Fig 4 Nusselt number for* A = *10*, Ra = *1* × *10*$^5$ *and* Da = *1* × *10*$^{-3}$

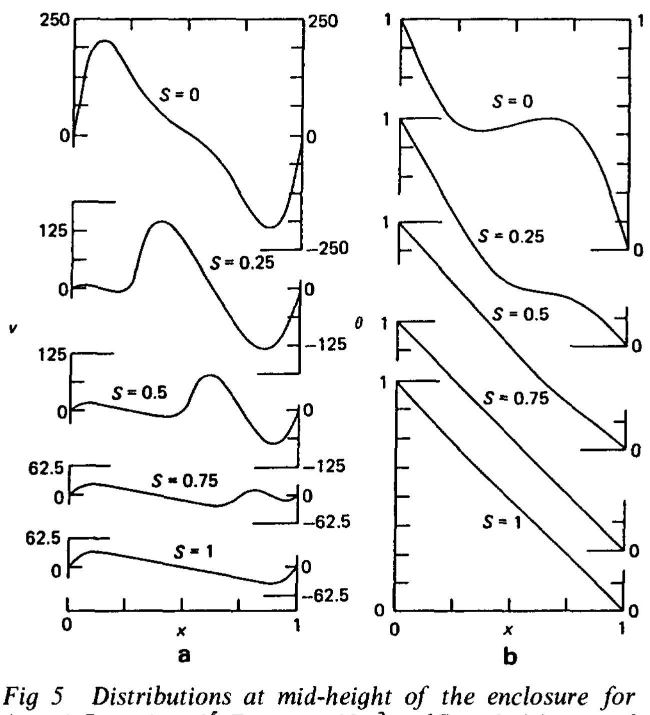


*Fig 5 Distributions at mid-height of the enclosure for* A = *10*, Ra = *1* × *10*$^5$, Da = *1* × *10*$^{-3}$ *and* $R_c$ = *1*: *(a) vertical velocity; (b) temperature*

*Ra*. From these figures, it is again seen that there is no need to fill the entire enclosure to achieve the best insulating result. For the same reason mentioned in the preceding paragraph, a (20 + 20) × 20 grid was used to obtain the results for $S = 0$ and $A = 5$ in Figs 7 and 9, and those for $S = 1$ in Fig 9.

Since the Brinkman-extended Darcy model has been used to generate the results, it is of interest to see how the results would compare with those from the pure Darcy model. Table 3 shows a comparison between the Brinkman results for $S = 1$ and those reported by Shiralkar *et al*[14] using the pure Darcy formulation. The results indicate that the Brinkman *Nu* incfeases as *Da* decreases and approaches an asymptotic value. This trend has also been observed by Tong and Subramanian[25] in an

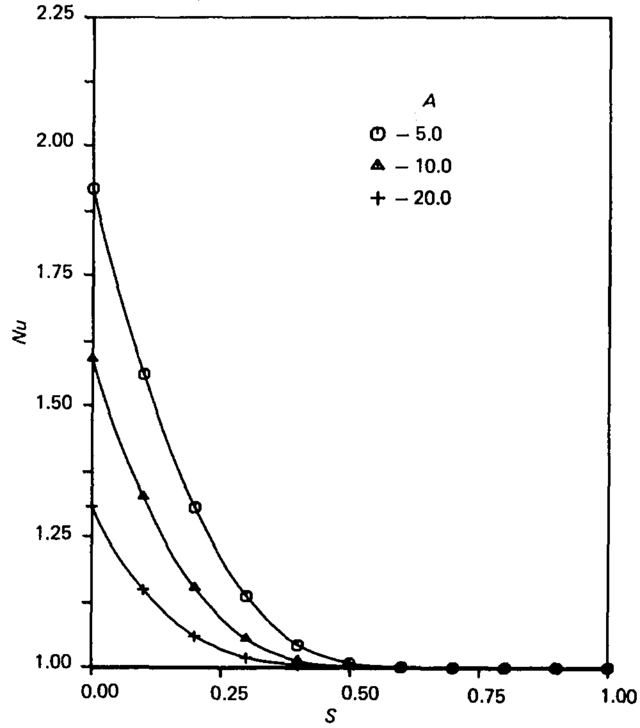


*Fig 6 Nusselt number for* Ra = *1* × *10*$^4$, Da = *1* × *10*$^{-7}$ *and* $R_c$ = *1*, ($Ra_o$ = *1* × *10*$^{-3}$)

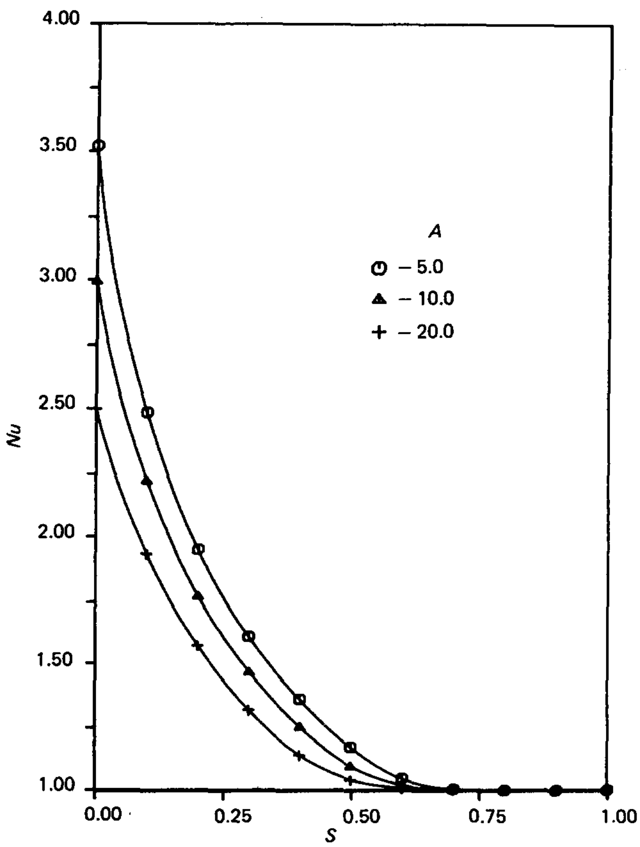


*Fig 7 Nusselt number for* Ra = *1* × *10*$^5$, Da = *1* × *10*$^{-7}$ *and* $R_c$ = *1*, ($Ra_o$ = *1* × *10*$^{-2}$)

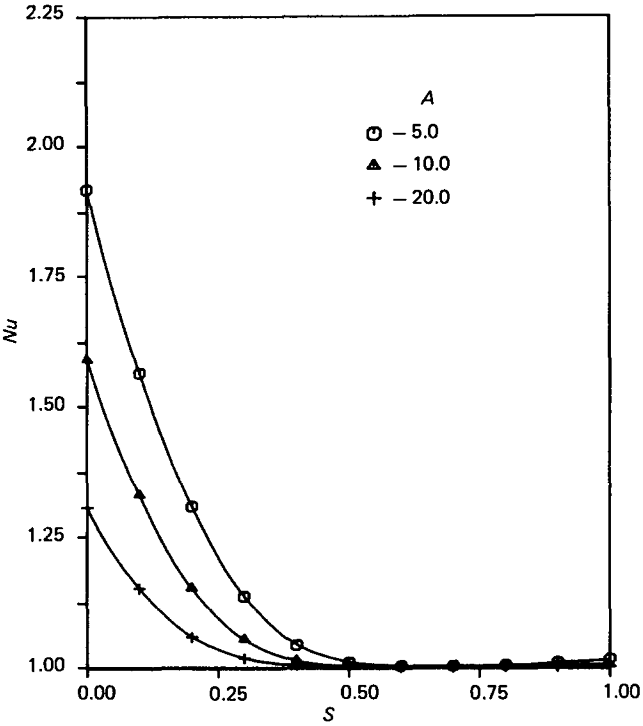


*Fig 8 Nusselt number for* $Ra = 1 \times 10^4$, $Da = 1 \times 10^{-3}$ *and* $R_c = 1$, $(Ra_o = 10)$

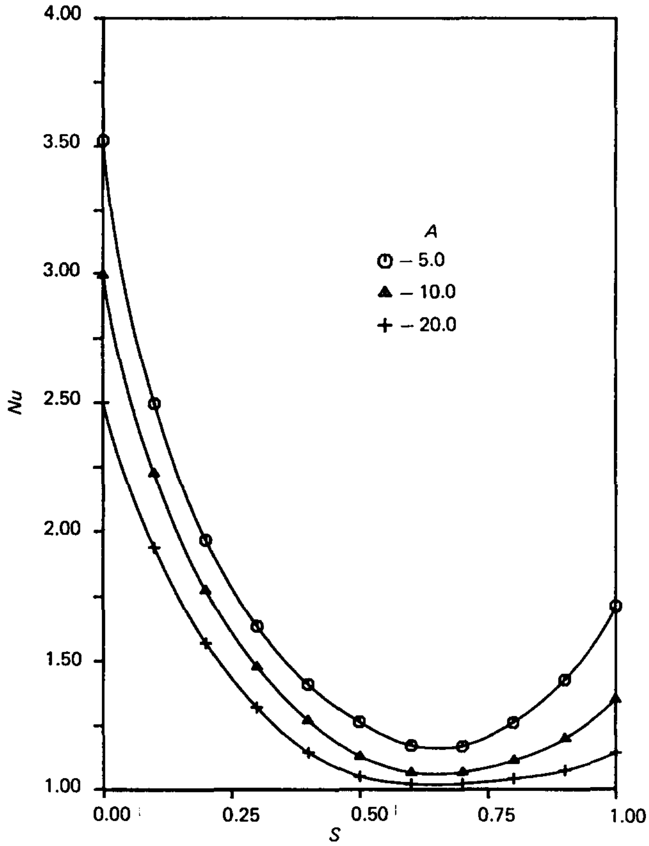


*Fig 9 Nusselt number for* $Ra = 1 \times 10^5$, $Da = 1 \times 10^{-3}$ *and* $R_c = 1$, $(Ra_o = 1 \times 10^2)$

**Table 3 Brinkman's effect for $S = 1$**

| | | *Nu* | | | | |
|---|---|---|---|---|---|---|
| | | Present, with Brinkmann's extension* | | | | Pure Darcy formulation |
| *A* | $Ra_0$ | $Da = 1 \times 10^{-3}$ | $1 \times 10^{-4}$ | $1 \times 10^{-5}$ | $1 \times 10^{-7}$ | Shiralkar *et al.*[14] |
| 5 | 50 | 1.34 | 1.41 | 1.42 | 1.42 | |
| | 100 | 1.77 | 1.93 | 1.95 | 1.96 | 2.09 |
| 10 | 50 | 1.16 | 1.19 | 1.20 | 1.20 | 1.25 |
| | 100 | 1.39 | 1.47 | 1.48 | 1.48 | 1.57 |

* *Results obtained with a* $(32+0) \times 32$ *grid*

analytical study of flow in the boundary-layer regime. The asymptotic value, in principle, should be the pure Darcy *Nu* because in the limit when $Da \to 0$, the Brinkman-extended model reduces to the pure Darcy model. The Brinkman results for $Da = 1 \times 10^{-7}$ differ from the pure Darcy results by no more than 6%. Also, the Brinkman results are already relatively constant when $Da \leqslant 1 \times 10^{-4}$.

## Conclusions

The problem of natural convective heat transfer in rectangular enclosures containing different amounts of porous insulation has been investigated. The formulation of the transport problem was based on the Brinkman-extended Darcy model. Finite-difference results have been obtained for heat transfer as a function of the governing parameters. It was found that under many circumstances there was no need to fill an enclosure completely with a porous material to achieve the best insulating effect. This implies that a better optimized insulation usage is possible.

## Acknowledgements

The authors are grateful for the support of this work by the National Science Foundation through grant DME-8105951. The authors would also like to thank Mr S. Orangi for performing some of the numerical calculations.

## References

1. **Elder J. W.** Numerical experiments with free convection in a vertical slot. *J. Fluid Mech., 1966*, **24**, *823–843*
2. **Wilkes J. O. and Churchill S. W.** The finite-difference computation of natural convection in a rectangular enclosure. *AIChE J., 1966*, **12**, *161–166*
3. **Newell M. E. and Schmidt F. W.** Heat transfer by laminar natural convection within rectangular enclosures. *J. Heat Transfer, 1970*, **92**, *159–168*

4. **MacGregor R. K. and Emery A. F.** Free convection through vertical plane layers—moderate and high Prandtl number fluids. *J. Heat Transfer, 1969,* **91**, *391–503*

5. **Ostrach S.** Natural convection in enclosures. *Advances in Heat Transfer, 1972,* **8**, *161–227*

6. **Raithby G. D. and Wong H. H.** Heat transfer by natural convection across vertical air layers. *Numerical Heat Transfer, 1981,* **4**, *447–457*

7. **Bankvall C. G.** Natural convection heat transfer in insulated structures, *1972, Report,* **38**, *Lund Institute of Technology*

8. **Chan B. K. C., Ivey C. M. and Barry J. M.** Natural convection in enclosed porous media with rectangular boundaries. *J. Heat Transfer, 1970,* **92**, *21–27*

9. **Burns P. J., Chow L. C. and Tien C. L.** Convection in a vertical slot filled with porous insulation. *Int. J. Heat Mass Transfer, 1977,* **97**, *449–474*

10. **Walker K. L. and Homsy G. M.** Convection in a porous cavity. *J. Fluid Mech., 1978,* **97**, *449–474*

11. **Bejan A.** On the boundary layer regime in a vertical enclosure filled with a porous medium. *Letters in Heat and Mass Transfer, 1979,* **6**, *93–102*

12. **Blythe P. A. and Simpkins P. G.** Convection in a porous layer for a temperature dependent viscosity. *Int. J. Heat Mass Transfer, 1981,* **24**, *497–506*

13. **Hickox C. E. and Gartling D. K.** A numerical study of natural convection in a horizontal porous layer subjected to an end-to-end temperature difference. *J. Heat Transfer, 1981,* **103**, *797–802 802*

14. **Shiralkar G. S., Haajizadeh M. and Tien C. L.** Numerical study of high Rayleigh number convection in a vertical porous enclosure. *Numerical Heat Transfer, 1983,* **6**, *223–234*

15. **Tong T. W., Birkebak R. C. and Enoch I. E.** Thermal radiation, convection and conduction in porous media contained in vertical enclosures. *J. Heat Transfer, 1983,* **105**, *414–418*

16. **Lock G. S. H. and Ko R. S.** Coupling through a wall between two free convection systems. *Int. J. Heat Mass Transfer, 1973,* **16**, *2087–2096*

17. **Viskanta R. and Lankford D. W.** Coupling of heat transfer between two natural convection systems separated by a vertical wall. *Int. J. Heat Mass Transfer, 1981,* **24**, *1171–1177*

18. **Anderson R. and Bejan A.** Heat transfer through single and double vertical walls in natural convection: theory and experiment. *Int. J. Heat Mass Transfer, 1981,* **24**, *1611–1620 1620*

19. **Bejan A. and Anderson R.** Heat transfer across a vertical impermeable partition imbedded in porous medium. *Int. J. Heat Mass Transfer, 1981,* **24**, *1237–1245*

20. **Vafai K. and Tien C. L.** Boundary and inertial effects on flow and heat transfer in porous media. *Int. J. Heat Mass Transfer, 1981,* **25**, *195–203*

21. **Neale G. and Nader W.** Practical significance of Brinkman's extension of Darcy's law: coupled parallel flows within a channel and a bounding porous medium. *Canadian J. Chem. Eng., 1974,* **52**, *475–478*

22. **Lundgren T. S.** Slow flow through stationary random beds and suspensions of spheres. *J. Fluid Mech., 1972,* **51**, *273–299*

23. **Neale G., Epstein N. and Nader W.** Creeping flow relative to permeable spheres. *Chem. Eng. Sci., 1973,* **28**, *1865–1874 1874*

24. **Spielman L. and Goren S. L.** Model for predicting pressure drop and filtration efficiency in fibrous media. *Environmental Sci. and Technol., 1968,* **2**, *279–287*

25. **Tong T. W. and Subramanian E.** A boundary-layer analysis for natural convection in vertical porous enclosures—use of the Brinkman-extended Darcy model. *Int. J. Heat Mass Transfer, 1985,* **28**, *563–571*

## Forthcoming articles

Transient conduction in a plate cooled by free convection
*T. W. Davies and D. R. E. Worthington*

LDA investigation of the turbulent flow around cylindrical obstacles on a rough surface
*F. K. Lim and A. K. Lewkowicz*

Effects of secondary flow on particle motion and erosion
*A. F. El-Sayed, R. Lesser and W. T. Rouleau*

Generation of nearly isotropic turbulence downstream of streamwise tube bundles
*P. E. Roach*

Velocity profile measurement by ultrasound Doppler shift method
*Y. Takeda*

On average heat transfer co-efficient – Technical note
*H. Barrow*

Statistical characteristics of intermittent liquid film flow
*M. A. Hounkanlin and P. Dumargue*

ADI method for MHD heat transfer in $r\theta z$ geometry with discontinuity in wall temperature
*B. Singh and P. K. Agarwal*

Multi-point optical measurement of simultaneous vectors in unsteady flow
*R. Adrian*

Investigation into turbulent developing flow in the entrance to a smooth pipe
*L. A. Salami*

Convective transfer from a transverse fin array exposed to two-dimensional turbulent flow
*A. T. R. Tindall and E. A. Vallis*

Turbulence enhancement of stagnation point heat transfer on a circular cylinder
*G. K. Hargrave, M. Fairweather and J. K. Kilham*

A comparison of experimental and predicted results for natural convection in an enclosure
*F. W. Schmidt, P. W. Giel, R. E. Phillips and D. G. Wang*

The local resistance of gas-liquid two-phase flow through an orifice
*C. Dekang, C. Zhihang, Z. Zaisan and Z. Ning*